

Mapping from structure to dynamics: A unified view of dynamical processes on networks

Jie Zhang,^{1,2,*} Changsong Zhou,^{3,†} Xiaoke Xu,⁴ and Michael Small¹

¹*Department of Electronic and Information Engineering, Hong Kong Polytechnic University, Hong Kong, People's Republic of China*

²*Centre for Computational Systems Biology, Fudan University, Shanghai, People's Republic of China*

³*Department of Physics, Center for Nonlinear Studies, Hong Kong Baptist University, Hong Kong, People's Republic of China*

⁴*School of Communication and Electronic Engineering, Qingdao Technological University, Qingdao, People's Republic of China*

(Received 15 August 2009; revised manuscript received 19 July 2010; published 27 August 2010)

Although it is unambiguously agreed that structure plays a fundamental role in shaping the collective dynamics of complex systems, how structure determines dynamics exactly still remains unclear. We investigate a general computational transformation by which we can map the network topology directly to the dynamical patterns emergent on it—independent of the nature of the dynamical processes. Remarkably, we find that many seemingly different dynamical processes on networks, such as coupled oscillators, ensemble neuron firing, epidemic spreading and diffusion can all be understood and unified through this same procedure. Utilizing the inherent multiscale nature of this structure-dynamics transformation, we further define a multiscale complexity measure, which can quantify the functional diversity a general network can support at different organization levels using only its structure. We find that a wide variety of topological features observed in real networks, such as modularity, hierarchy, degree heterogeneity and mixing all result in higher complexity. This result suggests that the demand for functional diversity is driving the structural evolution of physical networks.

DOI: [10.1103/PhysRevE.82.026116](https://doi.org/10.1103/PhysRevE.82.026116)

PACS number(s): 89.75.Hc, 05.45.Xt, 89.75.Fb

I. INTRODUCTION

The advances in the realm of complex networks have furnished us with a new paradigm to understand and characterize complex systems [1–3]. A large variety of real-world systems, from the human brain that is composed of billions of neurons, to our society, a collection of six billion cooperating individuals, can all be represented as complex networks. The discovery of scale free [4] and the small-world [5] structures has fundamentally altered our view of these networks. A variety of other topological features, such as clustering [6], hierarchical ordering [7], and degree mixing [8,9], are also emerging as important to the overall behavior of network systems. However, recent progress mainly focuses on the underlying topological structure [1], the effort to understand the system's dynamics or function has been less advanced [2,3,10–15].

With the increasing capability to capture simultaneously the time dependent activity of many components from complex systems [16] (such as the multiple electrode recording of neuronal populations [17], gene expression patterns [18], and time-resolved email correspondence [19]), unraveling the intricate relationship between the structure of a network and its dynamical behavior has become a problem of utmost importance, and hints toward the general organizing principles and a deeper understanding of complexity. Generally, the topological descriptors fail to capture the dynamical aspects explicitly. To characterize the dynamics of a network, it must be implemented as a dynamical system via extensive numerical simulations.

In this paper we seek a methodology to understand and predict the dynamical correlation among the components of a

complex system *directly through the underlying topology*. This is achieved by constructing the *node interaction profiles* through a tunable kernel function, which identifies the functional role of each node and all interaction pathways in a multiscale manner. The dynamical correlation among the units (or correlation pattern) is usually obtained by calculating the correlation index among the output time series from the components, and it underlies the functionality of a complex system. It has been intensively studied in chaos community and brain research groups, under either the banner of synchronization [20–22] or *functional* connectivity [23,24]. For example, it has been suggested that specific correlation patterns within large populations of neurons in the cortex are responsible for perception and cognition [25].

Barabási recently points out that various dynamical processes may share some common characteristics, which need to be unveiled possibly by new frameworks [26]. Interestingly, we find that our methodology is *independent of the details of the dynamical process*. Various processes on networks such as synchronization of coupled oscillators, ensemble neuron firing and diffusion processes can all be unified under this theoretical picture, suggesting that some general rules may govern the overall dynamical behavior of the seemingly diverse complex systems. Based on this dynamics-structure transformation, we propose a multiscale complexity measure, which can evaluate the range of correlation patterns a network can possibly generate over different organization levels. We find that various topological features such as topological heterogeneity [4], modularity [6], hierarchy [7] and nontrivial correlation [8] all translate into higher complexity, indicating that the need for multiple function governs the structural evolution of physical networks.

II. METHOD: MAPPING FROM STRUCTURE TO DYNAMICS USING KERNEL FUNCTION

Consider a complex system composed of N coupled dynamical units, whose equations are described by [20]: \dot{x}_i

*jzhang080@gmail.com

†cszhou@hkbu.edu.hk

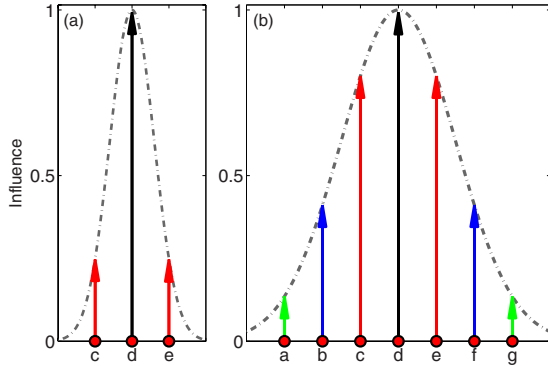


FIG. 1. (Color online) Modeling influence attenuation versus shortest distance by seeding a “kernel” function at the node (we take node d as an example). (a) Node d will have impact only on its immediate neighbors c and e under a small kernel bandwidth ($h=0.1$). (b) Node d can affect its higher-order neighbors like b and f under a large bandwidth ($h=1.5$).

$=F(x_i) + \sigma \sum_{j=1}^N A_{ij} H(x_j)$, $i=1, 2, \dots, N$ where $\dot{x}_i = F(x_i)$ governs the dynamics of each component, H is a fixed output function, σ represents the coupling strength, and A is the adjacency matrix of the underlying network. The problem is now, given only the topology A of the network, can we infer qualitatively the dynamical correlation among the components (i.e., the correlation among the multiple output time series $x_i(t)$, $i=1, \dots, N$ from each component) without implementing the network as a dynamical system? If so, what does this tell us about the behavior of different dynamical units within the same network structure?

A fundamental feature of a complex system composed of multiple interacting components is the presence of interaction pathways across a wide range of spatial scales [27]. Take a network of coupled dynamical systems for example, a pair of nodes usually exert a stronger influence on each other when directly coupled (i.e., their shortest path distance l_{ij} is 1), while this influence tends to weaken for indirectly linked nodes due to intermediaries (i.e., $l_{ij} > 1$). To quantify the influence attenuation with shortest path distance l on a network, we adopt a simple, monotonically decreasing function known as a kernel K (see Fig. 1) [28,29]. For a pair of nodes i and j , we then define their effective interaction R_{ij} , in the form of $K(l_{ij}, h)$, where l_{ij} is their shortest path distance, K is a non-negative, symmetric kernel function satisfying $\int_R K(l) dl = 1$, $\int_R l K(l) dl = 0$, $\lim_{l \rightarrow \infty} K(l) = 0$, and h is the *bandwidth* that controls the width of the kernel. For Gaussian kernel, the interaction matrix R will read: $R_{ij} = \exp(-l_{ij}^2 / 2h^2)$.

To predict the dynamical correlation among units, we should not only identify the effective influence among them, but also distinguish their specific roles in shaping the dynamics of others. Note that the i th column of R , R_i portrays the *effective interaction node i receives* from all its neighbors, which we call *interaction profile of node i* (We normalize the interaction matrix R so that each row sums to 1, indicating that each node exerts similar amount of influence to others). This vectorial profile systematically encodes the influence from all neighbors of node i as distinct driving forces (with their strengths determined by the kernel function) to its own

dynamics. Therefore R_i fully defines the unique “status” of node i . To further predict the dynamical correlation or functional connectivity F_{ij} between node i and j , we can calculate the similarity between their interaction profiles R_i and R_j : $F_{ij} = \frac{R_i \cdot R_j}{|R_i| |R_j|}$.

Here F_{ij} provides a unique clue to evaluate the dynamical correlation between the components. Unit i and j subject to a large number of common inputs (up to higher orders) are more likely to behave similarly. In this case, their profiles R_i and R_j will largely coincide by sharing many common entries, leading to a large F_{ij} —approaching 1. Conversely, a pair of units with few common drives tends to be independent and thus have a F_{ij} near 0. A great advantage of using kernel function lies in its adjustable bandwidth h , which can evaluate different levels of organization of a network and has concrete physical meanings for various dynamical processes on networks. In the following we will demonstrate how the correlation patterns in various dynamical processes can be inferred using the above mapping from structure A to dynamics F .

III. NUMERICAL VERIFICATION FOR DIFFERENT DYNAMICAL PROCESSES ON NETWORKS

A. Synchronization of coupled phase oscillators

We start with synchronization phenomena, which are widely observed in nature and occupy a privileged position in the understanding of emergent collective behavior across various contexts: neuroscience, ecology, biology, and engineering [21]. Recently the interplay between a network’s structure and its synchronization dynamics has attracted significant attention [22,30,31]. Here we use the Kuramoto model defined on various networks as a prototype example. It is governed by $\dot{\theta}_i = \omega_i + \frac{\sigma}{k} A_{ij} \sum_{j=1}^N \sin(\theta_j - \theta_i)$, $i=1, 2, \dots, N$, where ω_i is the frequency of phase oscillators [uniformly distributed in $(0,1)$], σ is coupling strength, A is the adjacency matrix, and \bar{k} is mean degree. Specifically, we will show that F_{ij} obtained at different kernel bandwidth h can provide a good estimation of the correlation patterns emergent under different σ .

With a small coupling σ , the oscillators are mostly independent. The dynamical distance between outputs of node i and j , defined as $D_{ij} = \langle \theta_i(t) - \theta_j(t) \rangle$ ($\theta(t)$ are wrapped to $[0, 2\pi]$ and $\langle \cdot \rangle$ means time average) will be nonzero and constitute a narrow distribution. When σ is large, the whole network reaches complete synchronization, and D_{ij} distribution will be a narrow peak again near 0. For intermediate σ , various functional clusters are formed, with D_{ij} distribution broadening [32]. We find that the D_{ij} distributions at various σ are exactly reproduced by F_{ij} with different h , see Fig. 2. At a small h , all entries in R_i are almost 0 except the i th, meaning each node only has impact on itself. The R_i s are mostly orthogonal, thus F_{ij} will centralize at 0. By contrast, the kernel becomes flat at a large h , leading every node to exert similar influence on all others. The F_{ij} then concentrates near 1 as all R_i s are almost identical. For medium h , the distribution of F_{ij} broadens within $[0,1]$ with the peaks corresponding to the formed functional clusters.

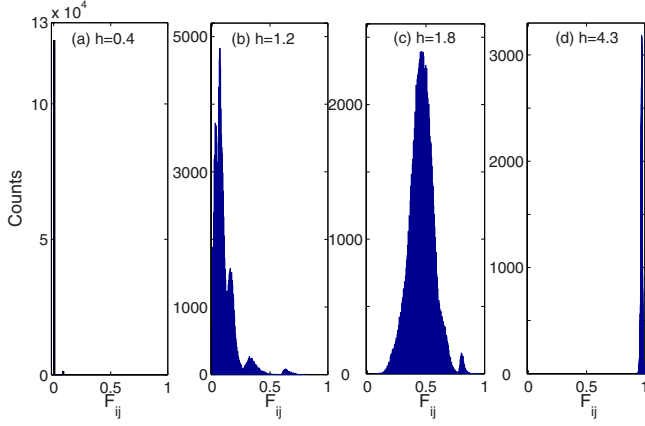


FIG. 2. (Color online) The distribution of F_{ij} for a random ER network (with 500 nodes and mean degree being 5) obtained at different bandwidth h . As can be seen, F_{ij} distribution broadens at a medium h , while shrinks at both small and large h , which has a good correspondence to coupling σ .

These examples show that the kernel bandwidth h is playing a role directly analogous to coupling strength σ . To further verify the consistency between F_{ij} and D_{ij} , we first get D_{ij} by implementing phase oscillators on a random network and a modular collaboration network [33]. We then calculate the correlation coefficient ρ between D_{ij} and $1-F_{ij}$ obtained at various h , see Fig. 3 (we use $1-F_{ij}$ because it is a dissimilarity measure that is consistent with D_{ij} , while F_{ij} is a similarity measure). We find that for a given σ , there is always an optimal kernel bandwidth h_{max} that attains a maximum similarity between D_{ij} and $1-F_{ij}$, with h_{max} and σ being positively correlated. The matrices D_{ij} and $1-F_{ij}$ demonstrate very similar patterns (see Fig. 4), reflected by a large correlation coefficient ρ between them. We find that ρ generally takes a large value for medium and high coupling σ , where oscillators have self-organized into well-defined clusters. For weak σ , the oscillators remains independent, thus D_{ij} is almost random and cannot be accurately fitted by F_{ij} .

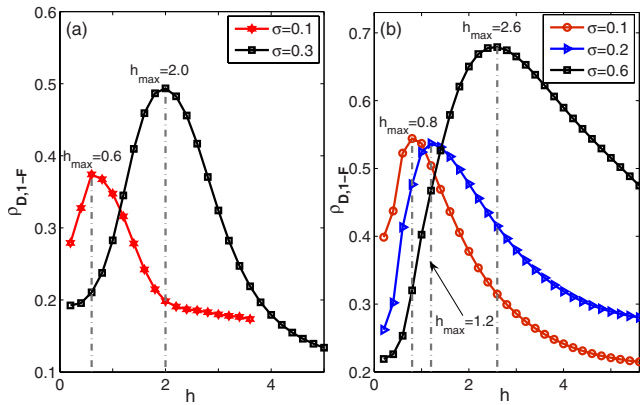


FIG. 3. (Color online) The correlation coefficient ρ between D_{ij} and $1-F_{ij}$ for coupled phase oscillator on (a) random (ER) network with 500 nodes (mean degree is 5) and (b) a collaboration network with 379 nodes, where nodes are scientists who conduct research on networks and links represent coauthorship [33].

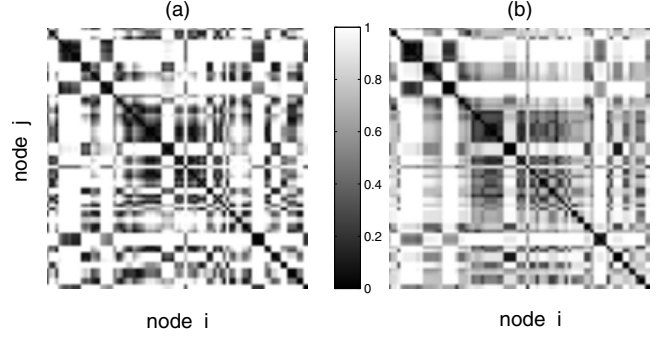


FIG. 4. Visualization of matrixes (a) D_{ij} and (b) $1-F_{ij}$ obtained from Fig. 3(b), i.e., phase oscillators on collaboration network, with $\sigma=0.6$ in computing D_{ij} and $h=2.6$ for F_{ij} . We show only a portion of the whole matrix for clarity.

B. Ensemble neuron firing of neural networks

Now we turn to a specific example in neuroscience, the coupled neurons in the cortex which communicate by nonsmooth, pulselike firings. The population dynamics of neurons, like the synchronous firing in the cortex, plays a fundamental role in cognitive functions of the brain [25,34,35] and is governed by the anatomy of the brain. Therefore understanding how connectivity influence the neural activity patterns (thus function) is of considerable importance in neuroscience. Here we try to assess the correlation patterns directly from the underlying structure. In particular, we couple the FitzHugh-Nagumo (FHN) neurons through real networks (by excitatory synapse with synaptic conductance g) to get D_{ij} first, and then check the correspondence between D_{ij} and F_{ij} . We use two networks possessing key properties of the cortex, i.e., small-world, hierarchical and modular structure. One is the neural network of *Caenorhabditis elegans* whose anatomy has been identified by biologist. The other is a hierarchically organized modular network [22] with two hierarchical levels. The network of FHN neurons is described by

$$\begin{cases} \varepsilon \dot{V}_i = V_i - V_i^3/3 - W_i + I_{ex} + I_i^{syn} \\ \dot{W}_i = V_i + a - b_i W_i + d \xi_i \\ I_i^{syn} = - \sum_{j \neq i}^N g A_{ij} s_j (V_i - V_{syn}) \end{cases}, \quad (1)$$

$i=1,2,\dots,N$, where V_i is the membrane potential, ξ_i is the i.i.d Gaussian noise (with zero mean and intensity d) representing the noisy background, and I_{ex} is the externally applied current. The parameter b , which uniformly distributes in $[0.45, 0.75]$, controls the single-neuron dynamics. The neuron undergoes Andronov-Hopf bifurcation at $b=0.45$, and have different excitability for $b>0.45$. Here the neurons are pulse-coupled by chemical synapses in an excitatory manner (the synaptic reversal potential V_{syn} is set as 0), with the synaptic variable s_j obeying $\dot{s}_j = \alpha(V_j)(1-s_j) - \beta s_j$, $\alpha(V_j) = \alpha_0/(1+e^{-V_j/V_{shp}})$.

The synaptic conductance g determines the amplitude of pulse conducted to postsynaptic neurons. It plays the same role as σ in coupled phase oscillators. The neurons fire almost randomly at a small g , and tend to form synchronous firing as g increases, giving rise to coherent oscillations. We

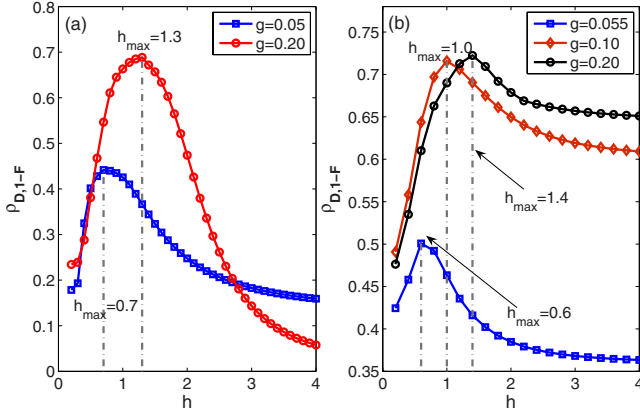


FIG. 5. (Color online) The correlation coefficient between D_{ij} and $1-F_{ij}$ for (a) *C. elegans* network with 297 neurons and each has 14 synaptic couplings on average. (b) Hierarchical network with 480 nodes [22]. Each node has 20 links to the most internal community (formed by 30 nodes), 2 links to the most external community (120 nodes that form four 30-nodes groups), and 1 more link to any other node. The parameters a and I_{ex} are set to be 0.7 and 0.05 in the simulation.

define the dynamical correlation among neurons as $D_{ij} = \langle \|f_i(n) - f_j(n)\| \rangle$, where $f_i(n)$ is the number of firings within time window n for neuron i (here the length of time window is 50 time steps). Alternatively, we can calculate $D_{ij} = \langle \|v_i(t) - v_j(t)\| \rangle$, where $v_i(t)$ is obtained by proper phase space reconstruction of $V_i(t)$. We find that F_{ij} obtained purely from network structure shows a high correlation with D_{ij} for both the *C. elegans* and the hierarchical network, see Fig. 5. Therefore we can evaluate the dynamics of neuronal populations directly from the anatomy. Moreover, the kernel bandwidth h plays a role similar to synaptic conductance g . For a given g , there is always an optimal bandwidth h_{max} under which F_{ij} best fits D_{ij} , and this h_{max} is positively correlated with g .

C. Epidemic spreading on networks

Triggered by the work of Pastor-Satorras *et al.* [36], there has been a revival of interest in understanding how network topology may affect epidemic propagation, wherein nodes represent individuals and the edges indicate connections through which infection can spread. Most current studies have only focused on the static, ensemble properties like the final infected numbers [37]. The dynamical evolution of the state of the individuals and their correlations remains less investigated. Here we consider the susceptible-infected-susceptible (SIS) model, in which the healthy node (susceptible) is infected with rate ν at each time step, and the infected can recover and become again susceptible with rate δ . This model is suitable to study the fluctuation of node dynamics, and the dynamics of node i is represented by a discrete-time stochastic process $S_i(t)$, with 1 indicating “infected” and 0 for “healthy.”

The correlation among the epidemic dynamics of the individuals can be defined as $D_{ij} = \langle \|S'_i(n) - S'_j(n)\| \rangle$, where $S'_i(n)$ is coarse grained from $S_i(t)$ by counting the number of

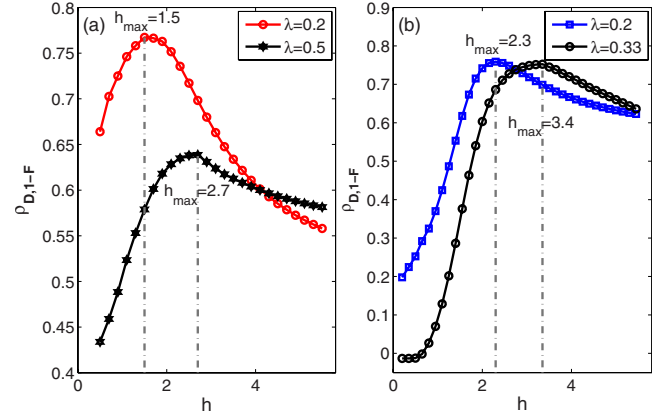


FIG. 6. (Color online) Correlation coefficient between D_{ij} and $1-F_{ij}$ for epidemic spreading on (a) scale free BA network (500 nodes with mean degree 5) and (b) a email correspondence network (1133 nodes).

1 in time window n . We find that D_{ij} is again nicely predicted by F_{ij} under a suitable h , see Fig. 6, where we run SIS models on two typical networks. Interestingly, we find h_{max} relates closely to the effective spreading rate $\lambda = \nu/\delta$, where ν and δ are infection and recovery rate, respectively. In Fig. 6 we see that node correlation at a small λ is optimally fitted by a kernel with small h , while correlation of the node dynamics under large λ is better reproduced by a wider kernel. This is because an infected node recovers quickly with a small λ , thus having a small range of influence fitted better with a small h . Conversely, a large λ makes the infected node persistently infective and has a large influence basin described well by a wider kernel.

D. Random walk on networks

Another fundamental dynamic process [38] on networks is the random walk, which relates to many practical problems on networks, such as navigability [39] and community detection [40]. Here we explore random walk on networks with particular attention to the correlation of the dynamics of the nodes. Here the “dynamics” of a node is encoded in the specific timings at which it is visited, which is fully described by a stochastic process $W_i(t)$, ($t=0, 1, 2, \dots, n$), with 1 represents “being visited” at time t and 0 otherwise.

The dynamical correlation of node i and j is then defined as: $D_{ij} = \langle \|W'_i(n) - W'_j(n)\| \rangle$ [$W'_i(n)$ is coarse grained from $W_i(t)$ by counting the number of 1 in each time window n], which is nicely predicted by F_{ij} , as is indicated by a large ρ between them (see Fig. 7). Here the random walk provides an ideal paradigm to validate our method as a mapping from structure to dynamics. Nodes sharing significant structural similarity [41] are more likely to be visited at the same time window, thus their “dynamics” will be highly correlated, which is precisely captured by our structure-dynamics transformation.

IV. UNIFYING VARIOUS DYNAMICAL PROCESSES ON NETWORKS

After demonstrating in Sec. III that the correlation patterns of various dynamical processes can be inferred by our

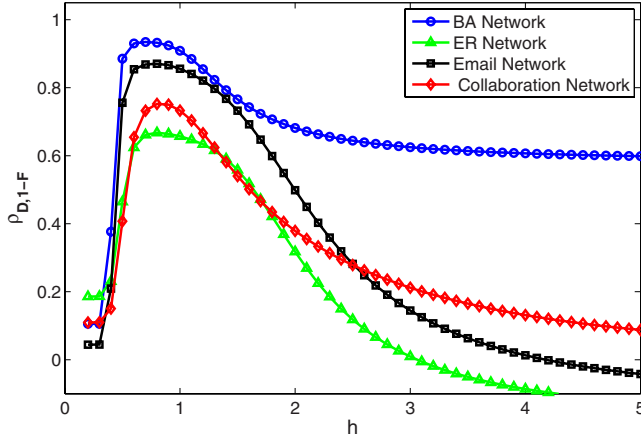


FIG. 7. (Color online) Correlation coefficient between D_{ij} and $1-F_{ij}$ for random walk on various networks. The Barabási-Albert and Erdős-Rényi network both have 1000 nodes, with mean degree being 20 and 10, respectively. The length of time window is 200.

mapping from A to F , it is then natural to consider what these processes on networks have in common. Figure 8 shows the functional relation between the optimal kernel bandwidth h_{max} and the physical parameters like σ for coupled oscillators, g for coupled neurons, and λ for epidemic spreading, which are obtained by simulating each dynamical process 50 times on a given network. A fundamental feature of these functional relations, as can be seen in Fig. 8, is their strict monotonicity, i.e., a wider kernel can be used to describe dynamical process with a larger coupling σ , conductance g , or effective spreading rate λ . This indicates that various dynamical processes on networks follow similar organization principles, and their dynamics can be understood and predicted by the same mapping from structure to dynamics. In order to predict exactly the dynamics on a network at a given physical parameter, we will need *a priori* knowledge of the functional relation shown in Fig. 8. Under the circum-

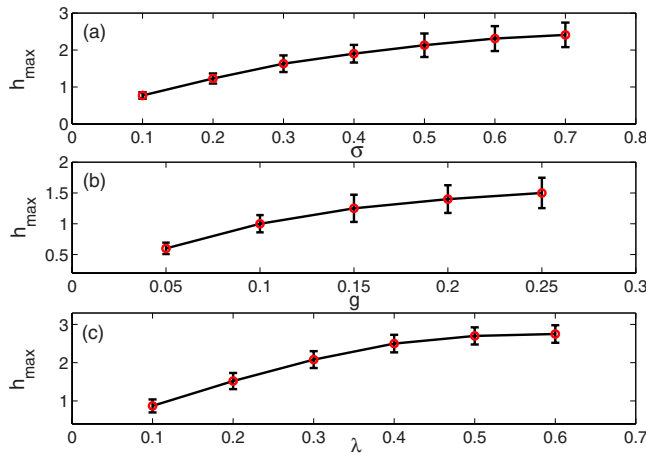


FIG. 8. (Color online) The relationship between optimal kernel bandwidth h_{max} and the key physical parameters of various dynamical processes on networks. (a) h_{max} and σ for coupled oscillators on collaboration network used in Fig. 3(b). (b) h_{max} and g for neural network used in Fig. 5(b). (c) h_{max} and λ for epidemic spreading on BA network used in Fig. 6(a).

stances that no *a priori* knowledge is available, we can still apply our mapping to a given network using kernels with a series of different width, which is expected to offer a full scan of the dynamics over a large range of physical parameters.

V. CHARACTERIZING COMPLEXITY OF COMPLEX NETWORKS: FROM STRUCTURE TO FUNCTION

Having established the mapping from network structure to its dynamics, we are naturally led to the questions: Why do real networks demonstrate distinctive features such as modularity, hierarchy, degree mixing, and heterogeneity? What are their roles in shaping the dynamics, or function of the network? Here we come up with a complexity measure by exploiting our structure-dynamics transformation, which can conveniently quantify how much function a network can support.

Understanding and quantifying complexity [32,42,43] has been an inherently interdisciplinary effort that spans a broad range of specialties. Sporns *et al.* proposed “neural complexity” to measure functional connectivity by implementing Gaussian dynamics [44] on networks. It has been shown that the correlation patterns lie at the core of functionality of a network [45–47]. Take coupled dynamical systems for example, both small and large couplings result in too narrow D_{ij} distribution to provide enough patterns of functional connectivity, while medium coupling induces broad D_{ij} distribution that may offer more choices of function (see Fig. 2). The richness of the correlation patterns (which is reflected by the broadness D_{ij} distribution) therefore determines the range of function a network can possibly support.

As we have shown in coupled oscillators, the dynamical correlation D_{ij} at various coupling strengths is well captured by F_{ij} at various h , thus we can approach the emergent correlation patterns directly from F_{ij} . Specifically, we use entropy H to characterize the broadness of F_{ij} distribution obtained at different h [$H(F) = -\sum_{k=1}^m p_k \log(p_k)$, where p_k is the probability that F_{ij} lies within bin k], which quantifies how much correlation pattern a network can possibly generate at various organization levels.

Figure 9(a) shows the complexity computed for typical networks at various scales. As can be seen, BA network shows a higher H than ER network at all scales, while assortatively and disassortatively mixed BA networks have higher H than BA networks. This is because scale free degree distribution and degree mixing can promote differentiation or facilitate the formation of various functional modules. Notably, we find that hierarchical and modular structures, which are widely observed in biological and social networks [7], demonstrate significantly higher complexity than their random counterparts, see Figs. 9(b) and 9(c). This is because the multiscale modular structure induces a wealth of correlation patterns persistently at different level of organization (corresponding to a wide range of h). The fact that all these distinctive topologies lead to higher complexity offers important insights into the evolutionary mechanism of real networks. This suggests that the demand for functional diversity is shaping the network architecture during the development of a physical network.

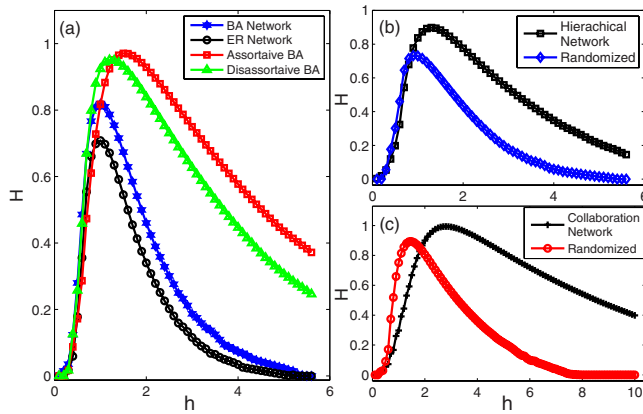


FIG. 9. (Color online) Multiscale entropy for (a) scale free BA, random ER network, assortatively and disassortatively mixed BA network. All networks have 1000 nodes and mean degree 20. (b) Hierarchical networks [used in Fig. 5(b)]. (c) Collaboration network [33]. Here we normalize H by a factor $H_m = \log(m)$, which is the entropy for uniform distribution, and m is the bin number.

VI. CONCLUSIONS AND DISCUSSIONS

In summary we have introduced an approach that can map the topological structure of a network directly to its dynamics. We demonstrate that this mapping offers a unified framework to account for the dynamical correlation emergent from seemingly different dynamical processes on networks, such as coupled oscillator, ensemble neuron firing and diffusion processes. A great advantage of our structure-dynamics transformation lies in its multiscale nature, which renders it especially useful for analyzing networks with hierarchical modular structure, such as metabolic and protein interaction networks [7].

For such networks, the modules that are usually present at small scale can be fitted by a relatively narrow kernel. Only

nodes within the same module interact, leading to a narrow F_{ij} distribution. Further up the scale these modules combine in a hierarchical manner, and F_{ij} distribution achieves the maximum at certain organization level h , indicating optimal division and cooperation among nodes. Finally, excessive widening of the kernel function will cause the nodes to appear homogenous. The multiscale modular organization in this case offers a wide range of scales at which segregation and integration combine to form diversified dynamical patterns, and does not depend on specific choice of kernels. Consequently the *multiscale structure* constitutes the structural basis for *multilevel function*. The reason why these networks are “complex networks” is that the multiscale structure can provide different levels of function persistently at different levels—and it is this property that is characterized by our multiscale entropy H .

Our approach can be directly extended to weighted and directed networks, and is computationally very effective. The time complexity of our mapping is bounded by $O(nl)$, where l is the largest shortest path distance of a network. Our mapping can furthermore be considered as a promising scheme to other problems like inverse engineering and controllability. The explicit relation between structure and dynamics will provide unique clues to infer the structure back from dynamical patterns, possibly with constraints like sparseness of connectivity. The control over the general networked systems can also be enhanced conveniently by locating the most sensitive nodes or links, the removal or rewiring of which would result in better network performance.

ACKNOWLEDGMENTS

This work is funded by Hong Kong Polytechnic University (G-YX0N). CS Zhou is supported by HK Baptist University.

- [1] R. Albert and A. Barabási, *Rev. Mod. Phys.* **74**, 47 (2002).
- [2] M. Newman, *SIAM Rev.* **45**, 167 (2003).
- [3] S. Boccaletti, V. Latora, Y. Moreno, M. Chavez, and D. Hwang, *Phys. Rep.* **424**, 175 (2006).
- [4] A. Barabási and R. Albert, *Science* **286**, 509 (1999).
- [5] D. Watts and S. Strogatz, *Nature (London)* **393**, 440 (1998).
- [6] M. E. J. Newman and M. Girvan, *Phys. Rev. E* **69**, 026113 (2004).
- [7] E. Ravasz, A. Somera, D. Mongru, Z. Oltvai, and A. Barabási, *Science* **297**, 1551 (2002).
- [8] M. E. J. Newman, *Phys. Rev. Lett.* **89**, 208701 (2002).
- [9] X. Xu, J. Zhang, J. Sun, and M. Small, *Phys. Rev. E* **80**, 056106 (2009).
- [10] A. Barrat, M. Barthélemy, and A. Vespignani, *Dynamical Processes on Complex Networks* (Cambridge University Press, New York, NY, 2008).
- [11] J. Ren, W. Wang, B. Li, and Y. Lai, *Phys. Rev. Lett.* **104**, 058701 (2010).
- [12] B. Barzel and O. Biham, *Phys. Rev. E* **80**, 046104 (2009).
- [13] R. Galán, *PLoS ONE* **3**, e2148 (2008).
- [14] J. Zhang and M. Small, *Phys. Rev. Lett.* **96**, 238701 (2006).
- [15] X. Xu, J. Zhang, and M. Small, *Proc. Natl. Acad. Sci.* **105**, 19601 (2008).
- [16] M. De Menezes and A. Barabási, *Phys. Rev. Lett.* **92**, 028701 (2004).
- [17] E. Brown, R. Kass, and P. Mitra, *Nat. Neurosci.* **7**, 456 (2004).
- [18] I. Golding, J. Paulsson, S. Zawilski, and E. Cox, *Cell* **123**, 1025 (2005).
- [19] A. Barabási, *Nature (London)* **435**, 207 (2005).
- [20] L. M. Pecora and T. L. Carroll, *Phys. Rev. Lett.* **80**, 2109 (1998).
- [21] A. Arenas, A. Díaz-Guilera, J. Kurths, Y. Moreno, and C. Zhou, *Phys. Rep.* **469**, 93 (2008).
- [22] A. Arenas, A. Diaz-Guilera, and C. Perez-Vicente, *Phys. Rev. Lett.* **96**, 114102 (2006).
- [23] E. Bullmore and O. Sporns, *Nat. Rev. Neurosci.* **10**, 186 (2009).
- [24] O. Sporns, D. Chialvo, M. Kaiser, and C. Hilgetag, *Trends Cogn. Sci.* **8**, 418 (2004).
- [25] F. Varela, J. Lachaux, E. Rodriguez, and J. Martinerie, *Nat.*

- [Rev. Neurosci. **2**, 229 \(2001\).](#)
- [26] A. Barabasi, [Science **325**, 412 \(2009\).](#)
- [27] J. Shao, S. V. Buldyrev, L. A. Braunstein, S. Havlin, and H. E. Stanley, [Phys. Rev. E **80**, 036105 \(2009\).](#)
- [28] J. Zhang, K. Zhang, X. Xu, C. Tse, and M. Small, [New J. Phys. **11**, 113003 \(2009\).](#)
- [29] K. Zhang and J. Kwok, [IEEE Trans. Neural Netw. **21**, 644 \(2010\).](#)
- [30] J. Gómez-Gardeñes, Y. Moreno, and A. Arenas, [Phys. Rev. Lett. **98**, 034101 \(2007\).](#)
- [31] E. Oh, K. Rho, H. Hong, and B. Kahng, [Phys. Rev. E **72**, 047101 \(2005\).](#)
- [32] M. Zhao, C. Zhou, Y. Chen, B. Hu, and B. Wang, [Phys. Rev. E \(to be published\).](#)
- [33] J. Park and M. E. J. Newman, [Phys. Rev. E **68**, 026112 \(2003\).](#)
- [34] P. Fries, J. Schroder, P. Roelfsema, W. Singer, and A. Engel, [J. Neurosci. **22**, 3739 \(2002\).](#)
- [35] G. Grinstein and R. Linsker, [Proc. Natl. Acad. Sci. U.S.A. **102**, 9948 \(2005\).](#)
- [36] R. Pastor-Satorras and A. Vespignani, [Phys. Rev. Lett. **86**, 3200 \(2001\).](#)
- [37] M. Barthélemy, A. Barrat, R. Pastor-Satorras, and A. Vespignani, [Phys. Rev. Lett. **92**, 178701 \(2004\).](#)
- [38] J. Noh and H. Rieger, [Phys. Rev. Lett. **92**, 118701 \(2004\).](#)
- [39] M. Boguñá, D. Krioukov, and K. Claffy, [Nat. Phys. **5**, 74 \(2009\).](#)
- [40] M. Rosvall and C. Bergstrom, [Proc. Natl. Acad. Sci. U.S.A. **105**, 1118 \(2008\).](#)
- [41] E. A. Leicht, P. Holme, and M. E. J. Newman, [Phys. Rev. E **73**, 026120 \(2006\).](#)
- [42] A. Barabási, [Nat. Phys. **1**, 68 \(2005\).](#)
- [43] T. Vicsek, [Nature \(London\) **418**, 131 \(2002\).](#)
- [44] O. Sporns, G. Tononi, and G. Edelman, [Cereb. Cortex **10**, 127 \(2000\).](#)
- [45] C. Stam, [Neurosci. Lett. **355**, 25 \(2004\).](#)
- [46] S. Dodel, J. Herrmann, and T. Geisel, [Neurocomputing **44-46**, 1065 \(2002\).](#)
- [47] V. M. Eguiluz, D. R. Chialvo, G. A. Cecchi, M. Baliki, and A. V. Apkarian, [Phys. Rev. Lett. **94**, 018102 \(2005\).](#)